Egypt. J. Chem. **Vol. 65**, No. 4 pp. 579 - 589 (2022)

Egyptian Journal of Chemistry

http://ejchem.journals.ekb.eg/

Synthesis of new polymers linked to heterocyclic using zinc oxide with nanostructures extracted from natural sources.

Khalida A. Thejeel[*], Sanaa A. Alsahib[**], Israa F. Ascar[**] and Muneer Abbas Hussein[***]

[*] *Department of Geophysics, College of Remote Sensing and Geophysics, Al-Karkh University for Science, Iraq.*

[**] *Department of Chemistry, College of Science for women, University of Baghdad, Baghdad, Iraq.*

[***] *The Ministry of Environment, Iraq.*

Abstract

This research has been directed towards the polymerization of heterocyclic compounds by the reaction it with acrylic acid to prepare new polymeric compounds using zinc oxide nanoparticles prepared from natural sources and used in various pharmaceutical, medical and industrial applications. Zinc oxide nanoparticles were prepared from natural plant sources and with a high product to be used as a catalyst to prepare industrially important monomers. These monomers contain a number of active groups that can be used by entering into a number of industrially important reactions with a very high production. Zinc oxide nanoparticles, monomers, and polymers were characterized using spectroscopy methods.

Keywords: Acrylic acid, Zinc oxide nanoparticles, Antibacterial activity, Cloves, Polymers, Heterocyclic, Plant extract.

1. Introduction

Due to the importance of polymers and their applications, and because of the rapid depletion of petroleum resources, the obvious alternative which lies in the great diversity of renewable raw materials and the design of more sustainable polymers to replace the classic materials and to prepare a number of important polymers using monoxides. In recent times, the importance of nano-oxides and their association in the preparation of many compounds important industrially and medically has emerged [1].

In this study, ZnONPs were prepared from locally available natural plant sources in inexpensive methods and with a high product to be used as a catalyst for preparing industrially important monomers. These monomers contain a number of effective groups that can be used by entering into a number of industrially important interactions with a very high product [2].

Nanotechnology is gaining increasing importance in many fields of research, as nanoparticles due to their small size acquire the task characteristics associated with the size of small particles [3]. This branch is considered qualified for the rapid growth of engineering and all sciences and medical fields, and fundamental work is carried out. The applications of metal nanoparticles have shown an interesting confrontation in industrial organic chemistry due to their exceptional chemical and physical properties. Earlier, many preparations were used using ZnO nanoparticles [4].

Nano-crystalline metal oxides such as Nano-zinc oxide show versatile applications as active gas adsorption or demolition of hazardous chemicals [5,6] and catalysts in various organic conversions [7] however the green formation of nanoparticles using natural seeds has great potential to increase the production of nanoparticles without the use of toxic and expensive chemicals. Due to the effective nature of its minimal toxicity, the mineral zinc is fundamentally important in treatment as an ideal antibacterial. At present, several studies confirm the anti-fungal, bacterial and anti-viral properties of spice plants [8].

Cloves are the flower buds of the clove tree, and it is an evergreen also known as *Syzygium aromaticum*. Found in both whole and ground forms, this versatile spice can be used.

Clove *(Syzygium aromaticum)* is one of the worthiest spices and has attracted great interest due to its strong antimicrobial and antioxidant activities that stand out among other spices. Natural phytochemicals such as phenolic compounds,

*Corresponding author e-mail: khalidathejeel@kus.edu.iq

Receive Date: 06 October 2021, Revise Date: 11 October 2021, Accept Date: 26 October 2021

DOI: 10.21608/EJCHEM.2021.92971.4644

©2022 National Information and Documentation Center (NIDOC)

alkaloids, flavonoids, inositol, tannins, terpenes, saponins, resins, vitamins, and amino acids [9,10].
Phytochemicals act as a strong reducing agent in nanoparticle compounds and are effective in forming ZnONPs. Plant extracts can remove various steps in nanoparticle compounds, acting as a natural reducing, stabilizing, and covering agent. Thus, not only cost reduction and utilization of chemical agents but also metallic compound nanoparticle agglomeration and oxidation-reduction [11,12].
Pyrazole derivatives are heterocyclic compounds recognized for possessing a wide range of biological activities and exhibiting important biological properties such as anti-inflammatory [13], antifungal [14] anticancer activity, antiviral, anti-tumor, antibacterial, andante-leukemiaa activity [15].

2.Experimental

2.1 Materials

The chemicals used in this study were supplied from Sigma- Aldrich, BDH and SDI (state company for drug industries and medical appliance) companies Aldrich and Fluka Companies (SDI) Samara–Iraq. Infrared spectra were recorded on KBr disk on SHIMADZU FT-IR-8300/ Japan; UV Perkin Elmer lambda 25, UV-VIS spectrophotometer Japan; NMR, 500MH_Z in DMSO-d_6. TGA sample robot, gas dosing system, vacuum, many different sample holders and crucibles for different applications temperature range: -150 up to 1000/ 1400/ 1600/ 1750/ 2000/ 2400°C Japan; DSC , Bruker Announces , UK-MSA; FESEM, Electron images were taken using Scanning Electron Microscope (Hitachi S3200 LV) ,1-3 drops of NP solution were drop casted on 0.5 x 0.5 cm piece of glass and then a very thin gold layer was coated using sputtering technique. japan; FETEM, UTM (RM400) (FETEM) Brand, JEOL Model, JEM-2100F Japan; EDS Bruker Announces UK-MSA,

2.2 Methods of synthesis

2.2.1 Preparing and extracting Nano-oxides from natural sources (clove)

Manufacturing nano-oxide by sedimentation method using chloride of zinc to be prepared as nano-oxide. After extracting it from the plant (clove), each component was dissolved in (100 ml) deionized water to form (0.1 M). The sodium hydroxide solution (0.1 M) was poured slowly with vigorous stirring until the pH reached 14. Black sediments were obtained and washed repeatedly with deionized water and absolute ethanol for several times until they reached a pH of 7. The washed sediments were then dried at 80 ° C for 16 hours. Finally, the nanostructured oxide aggregation was calculated at 500 ° C for 4 hours. It was investigated by x-ray dipstick (XRD) fig. (6,9). Morphology was monitored by electron microscopy (SEM) Fig. (7, 8). The chemical properties were examined by infrared spectroscopy.

2.2.2 Synthesis the monomer 3-amino-1-(4-(dimethylamino) phenyl)-5,10-dioxo-5,10-dihydro-1H-pyrazolo[1,2-b] phthalazine-2-carbonitrile 1 using Nano-oxide as a catalyst:

A mixture of dicyanomethane (0.066 g, 0.01 mole) and a suitable dihydrate) 4- (dimethylamino) benzaldehyde, propionaldehyde (0.01 mole) 5, 5-diethyl-2,3,5,8-tetrahydrophalazine -1,4 - Dione (0.220 g, 0.01 mole) and 10% mole nanoxide are placed in a container. Then the reaction mixture was heated at (80-100 ° C) for a period of (5-8 hours) and the procedure was carried out as monitored by TLC. Then the reaction mixture was cooled, washed with ethanol (2 x 3 mL) and evaporated under vacuum to give the complex product **1**.

2.2.3 Synthesis the monomer 1-(4-(dimethylamino) phenyl)-3-(2,5-dioxo-2,5-dihydro-1H-pyrrol-1-yl)-5,10-dioxo-5,10-dihydro-1H-pyrazolo[1,2-b] phthalazine-2-carboxylic acid 2.

A mixture of the compound **1**(0.359 gm, 1.001 mole) was added to (0.196 gm 1.0.01 mole) maleic anhydride. The mixture was dissolved with 10 ml of ethanol was added to 2 drops of sulphuric acid and the mixture was heated with stirring at (60-70 ° C) for 3 hours until all the materials were mixed until the dark brown liquid was formed. The solvent was evaporated under a vacuum to give the complex product **2**.

2.2.4 Synthesis the monomer 1-(4-(dimethylamino) phenyl)-3-(2,5-dioxo-2,5-dihydro-1H-pyrrol-1-yl)-5,10- dioxo-5,10-dihydro-1H-pyrazolo[1,2-b] phthalazine-2-carbonyl chloride 3

In a 150 mL flask, compound **2** (0.5 g, 0.023 mole), 20 mL of dimethyl sulfoxide (DMSO) and (0.034 mole) of thionyl chloride were placed and the mixture was mixed using a magnetic stirrer at 20 ° C, then Triethylamine (1.815 g, 0.0179 mole) was added after 20 minutes.

2.2.5 Synthesis the compound 1-(4-(dimethylamino) phenyl)-3-(2,5-dioxo-2,5-dihydro-1H-pyrrol-1-yl)-5,10-dioxo-N-(4-(N-(pyrimidin-2-yl) sulfamoyl) phenyl)-5,10-dihydro-1H-pyrazolo[1,2-b] phthalazine-2-reviewer 1carboxamide 4.

The[4-Amino-N-(2-primidinyl) benzenesulfon amide compound (0.575 g, 0.023 mole) was added to the reaction mixture from the previous step with stirring at 30 ° C for 30 minutes. The mixture was then cooled on ice, washed with ethanol, left until a precipitate, filtered and dried.

2.2.6 Synthesis polymers: poly [2-((1-(1-(4-(dimethylamino) phenyl)-5,10-dioxo-2-((4-(N-(pyrimidin-2-yl) sulfamoyl) phenyl) carbamoyl)-5,10-dihydro-1H-pyrazolo[1,2-b] phthalazin-3-yl)-2,5-dioxo-4-propylpyrrolidin-3-yl) methyl) butanoic acid] 5, and poly[2-((1-(1-ethyl-5,10-dioxo-2-((4-(N-(pyrimidin-2-yl) sulfamoyl) phenyl) carbamoyl)-5,10-dihydro-1H-pyrazolo[1,2-b] phthalazin-3-yl)-2,5-dioxo-4-propyl pyrrolidin-3-yl) methyl) butanoic acid] 6.

(0.02 g) of compound **4** was mixed with an excess amount form of acrylic acid with (10 ml) of toluene in a 50 ml in a round bottom, which was sealed and placed in a water bath at 90 ° C and two drops of methyl ethyl ketone were added. Peroxide (MEKP), then pass nitrogen gas from one of the nozzles of the vial. The reaction continued for 2-3 hours under reflux. At the end of the polymerization the solvent was evaporated, the precipitate was filtered, washed with diethyl ether, and finally dried in an oven at 50 ° C.

Table (1): Clarifies the diagnosis and physical properties of the intermediate and final compounds **1-6**.

Comp. No.	Yield %	Color	Recyst. Solvent	M.P ^{O}C
1	88	Brown	Ethanol	122-124
2	75	Dark Brown	Ethanol	176-178
3	77	Brown	DMF	240-242
4	79	Green	Ethanol	166-168
5	85	Yellowish green	Ethanol	220-222
6	89	Brown	DMF	232-234

3. Results and discussion

3.1 Characterization

UV–Visible spectrophotometer analysis

The solid white coloured samples of ZnONPs synthesized using chloride of the element were subjected to scan UV-Spectrophotometer in the range of 200–1000 nm. Various peaks were observed under UV region, peaks at 217.45 nm, 298.57 nm, 304.64 nm, 312.66 nm, 315.09 nm, 322.32 nm, 334.69 nm, 328.77nm, 345.09 nm, 351.50 nm and 352.75 nm for indicates the zinc oxide nanoparticles formation Fig. (1).

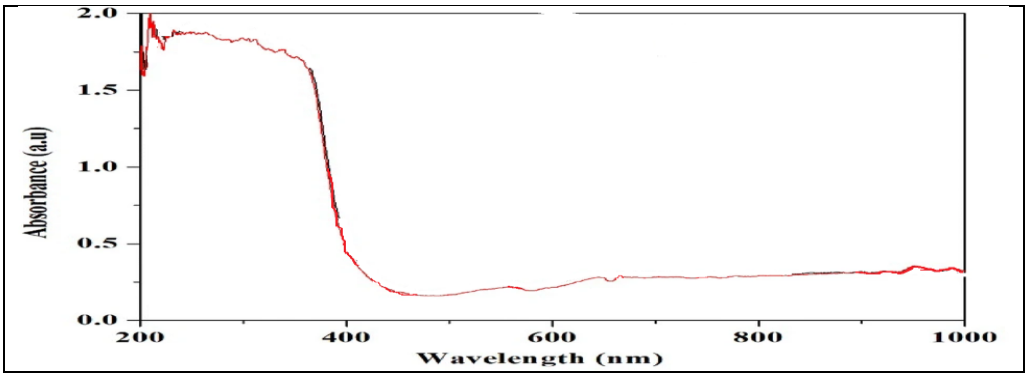

Fig. (1) UV–visible spectrophotometer analysis

X-Ray Diffraction analysis

Synthesized particles were subjected to X-Ray diffraction studies, to obtain the crystallinity and average particle size of synthesized nanoparticles. Following figures reveal the XRD pattern of zinc oxide nanoparticles. Number of Bragg reflections for ZnONPs using goat fecal matter appears at 2θ=31.77° (100), 34.44° (002),

36.27° (101), 46.52° (102), 56.93° (110), 61.86° (103), 67.05° (112), 68.12° (201) and 76.94 (202). which elucidates the hexagonal wurtzite structure which corresponds to pure zinc oxide nanoparticles. By using Debey-Scherrer equation, the average particle size of synthesized particles was calculated to be as 28.5 nm, which inwards suggests the formation of smaller particles size Fig. (2).

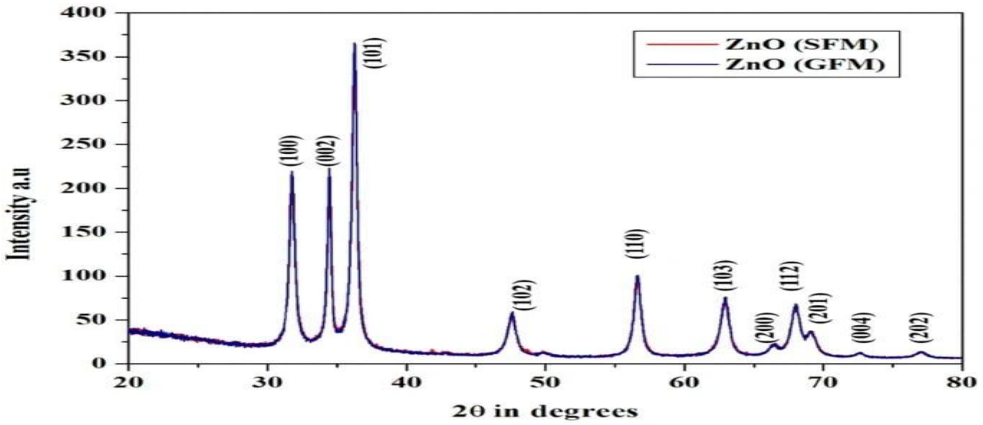

Fig. (2) XRD pattern of zinc oxide nanoparticles

Scanning electron microscope (SEM) analysis

SEM analysis is used to analyze the structural and morphological confirmation of synthesized nanoparticles Fig. 3 reveals the SEM image of ZnONPs. Particles clearly execute the spherical structural formation. In following image, we can clearly observe the obtained particles possess nearly spongy like and flower-like structural nanoparticles. Following figure, clearly observe oval like structured particles and flower-like structured irregularly formed particles. Nanoparticles exhibits lower particle size and possess nearly 40–130 nm .

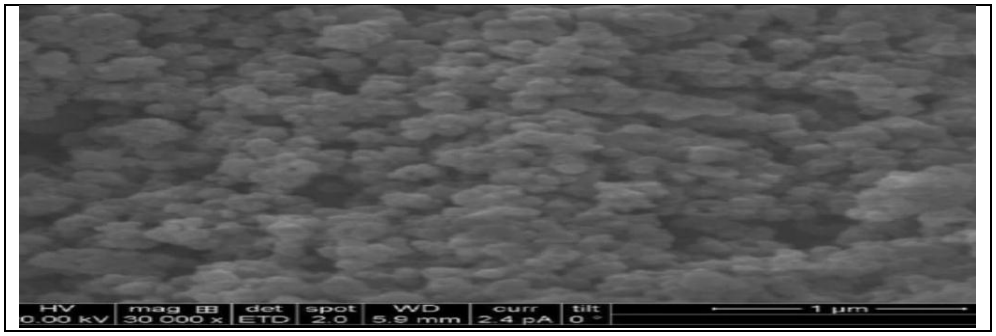

Fig. (3) The SEM image of ZnONPs

3.2 Chemistry

The final compounds and intermediate compounds were prepared starting from a tetrahydrophthalazine derivative and malononitrile with different parents (dimethyl aminobenzyldehyde, propionaldehyde) to produce the first compound **1a** which is an amino- different substituent - pyrazolophthalazine carbonate which is converted as after to the second compound **2** dinoxopyrrol -1-different substitution - pyrazolofthalazine is a carboxylic acid in its reaction with dihydrofuran and ethanol in the presence of the acid medium. The third compound acid chloride **3** was prepared from treating the second compound with a sulfone amide compound to produce the fourth compound **4**. The polymerization process of the last compound was carried out with acrylic acid to yield the final compounds **5** and **6**.

Synthetic pathways for newly prepared derivatives **1-6** are presented in scheme (1).

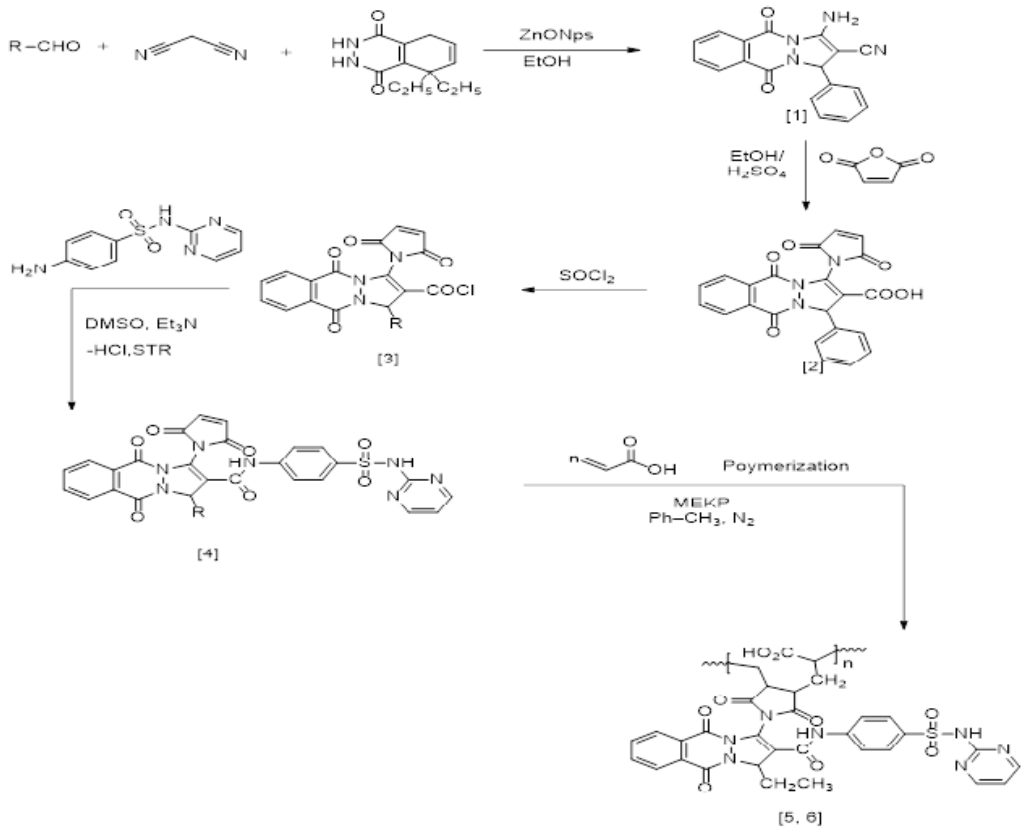

p

R: a= CH_3CH_2CHO & b= $(CH_3)_2NC_6H_4CHO$

n = number of monomers

Scheme 1: Synthetic pathways for prepared derivatives **1-6**.

FT-IR

Infrared spectral data of **1–6** from 400 - 4000 cm^{-1} as KBr are shown in Figures 4 and 5 and 6 summarized in Table (2). In compound **1**, ν(NH_2) is at 3444 cm^{-1} have been assigned to 1°−NH_2. As expected for compound **2** ν(OH) at 3216 cm^{-1}, and ν(CO)carboxylic at 1708 cm^{-1} which is higher than of ν(CO) in amide. compound **3** exhibit ν (CO) for acid chloride at 1780 cm^{-1}. Compound **4** gives ν (NH) at 3328, ν (C=N) at 1601 cm^{-1} and $\nu_{as.}$ (SO_2) at 1370 cm^{-1}. Compound **5** exhibit ν (OH) at 3274 cm^{-1} and ν (CO) carboxylic occurs at 1706 cm^{-1}.

Table (2): Illustrates the diagnosis of the effective groups by using infrared spectroscopy for the intermediate and final compounds **1-6**.

Compounds		Bands (cm^{-1})	Interpretation
[1]	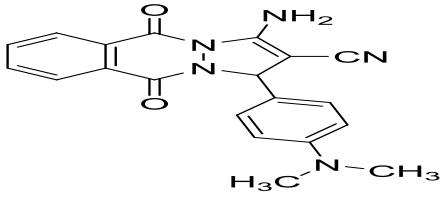	3444	ν (NH_2) Primary amine
		3062	ν (C-H) Aromatic
		2945	ν (C-H) Aliphatic
		2210	ν (CN) Nitrile
		1674	ν (C=O) Amide
		1559	ν(C=C) Aromatic

[2]

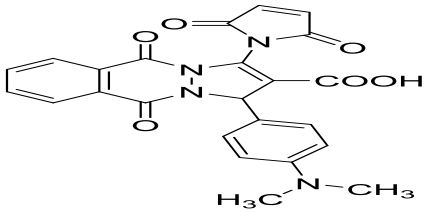

3216	ν (O-H)
3045	ν (C-H) Aromatic
2988	ν (C-H) Aliphatic
1708	ν (C=O) Carboxyl
1678	ν (C=O) Amide
1588	ν (C=C) Aromatic

[3]

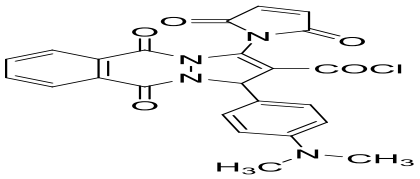

3056	ν (C-H) Aromatic
2971	ν (C-H) Aliphatic
1780	ν (C=O) Acid chloride
1679	ν (C=O) Amide
1578	ν (C=C) Aromatic

[4]

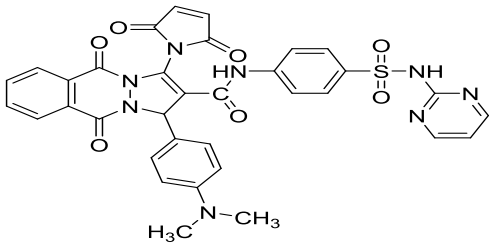

3328	ν (NH)
3061	ν (C-H) Aromatic
2945	ν (C-H) Aliphatic
1687	ν (C=O) Amide
1601	ν (C=N)
1558	ν (C=C) Aromatic
1370	ν (SO_2) Asym.

[5]

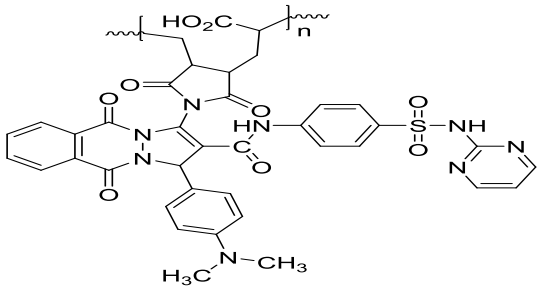

3381	*ν (NH)*
3274	*ν (OH)*
3056	*ν (C-H) Aromatic*
2962	*ν (C-H) Aliphatic*
1706	*ν (C=O) Carboxyl*
1688	*ν (C=O) Amide*
1606	*ν (C=N)*
1555	*ν (C=C) Aromatic*
1331	*ν (SO_2) Asym.*

[6]

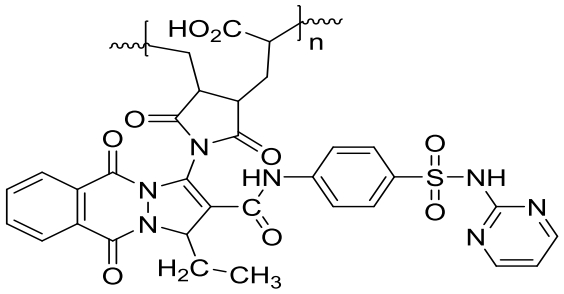

3350	ν (NH)
3250	ν (OH)
3059	ν (C-H) Aromatic
2988	ν (C-H) Aliphatic
1709	ν (C=O) Carboxyl
1685	ν (C=O) Amide
1597	ν (C=N)
1549	ν (C=C) Aromatic
1338	ν (SO_2) Asym.

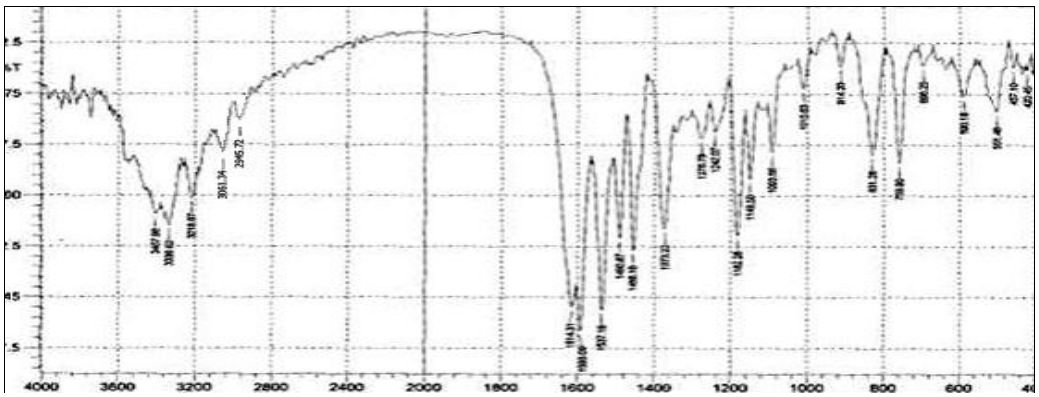

Fig. (4) Demonstrates the effective aggregates using the infrared spectroscopy of one of the intermediate compound **4**

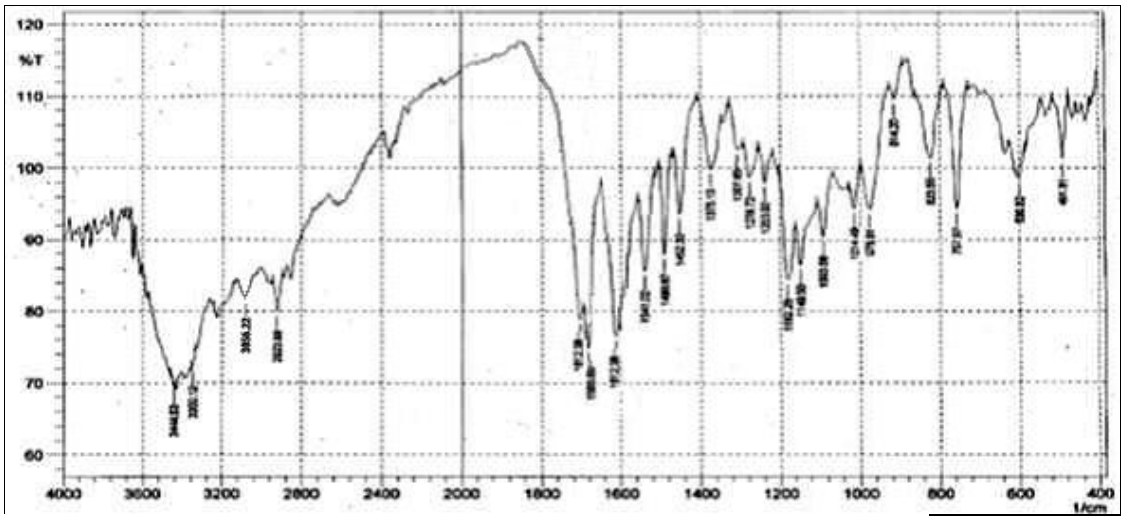

Fig. (5) Demonstrates the effective aggregates using the infrared spectroscopy of a compound **5.**

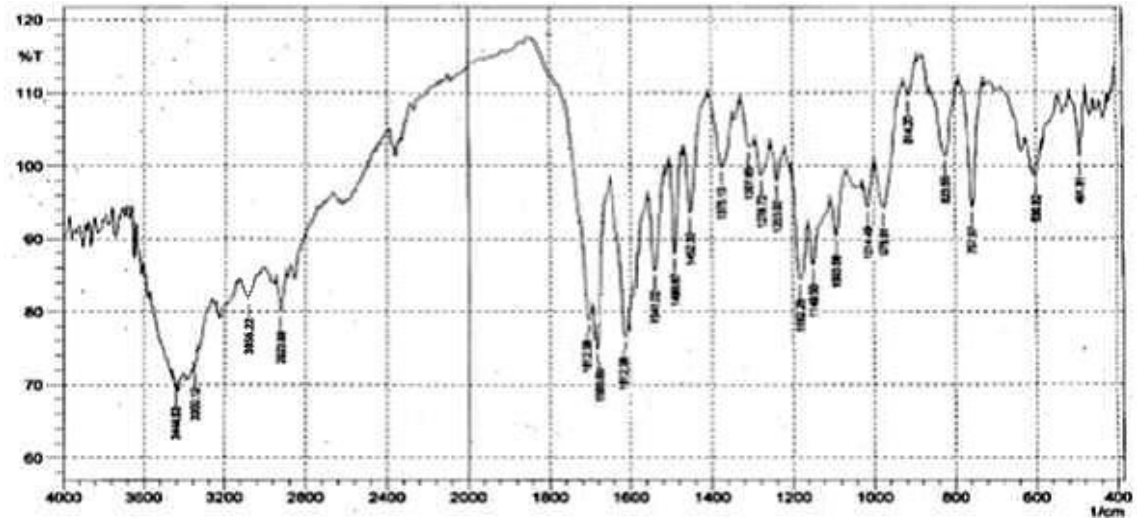

Fig. (6) Demonstrates the effective aggregates using the infrared spectroscopy of a compound **6**.

^{1}H- and ^{13}C –NMR

^{1}H NMR and ^{13}C NMR spectral data of 1–6 are listed in tables. The ^{1}H-NMR spectra of compound **1** showed the absence of the N-H in addition to appear chemical shift at 8.12ppm for NH_2, the ^{13}C-NMR spectrum of 44.72 ppm (C_{19}, C_{20}),63.34 ppm (C_1),116.52ppm (C_{12}), 121.55-134.42 ppm (C_2-C_9),(C_{13}-C_{18}),159.51 ppm (C_{10},C_{11}). In compound **2** the ^{1}H- and ^{13}C NMR spectra were noticed shift at ١١.34 ppm for OH, the ^{13}C-NMR spectrum 122.34-137.81 ppm (C_{22}, C_{23}),161.35 ppm (C_{21}, C_{24}). The ^{1}H-NMR spectra of compound **3** showed the absence of the O-H and ^{13}C NMR spectra were noticed chemical shift at 167.81 ppm for (C_{12}). The ^{1}H-NMR spectra of compound **4** showed the 9.44ppm (s,

1H, -CO-N<u>H</u>), 11.21ppm (s, 1H, -SO_2-N<u>H</u>), ^{13}C NMR spectra for (C_{25}-C_{34}) 118.11-139.89 ppm. The ^{1}H-NMR spectra for compounds **5** and **6** shown chemical shift between 10-24 to 10.90 ppm for (OH), ^{13}C NMR spectrum of **5** exhibit chemical shift at 35.44 (C_{35}, C_{36}, C_{38}) and 171.34 ppm for (C_{37}). ^{13}C NMR spectrum of 6 exhibit chemical shift at 36.21 (C_{30}, C_{31}, C_{33}),171.34 (C_{32}) for compound **6.** Table (3), Fig. (7,8, 9,10).

Table (3): Illustrates the diagnosis of the intermediate and final compounds (1-6) by using PPR.

Comp. No.	Compound structure with numbering of carbon atoms	^{1}H-NMR parameters δ (ppm)	^{13}C-NMR parameters δ (ppm)
1	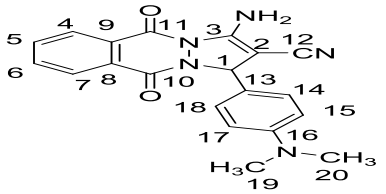	3.31 (s, 6H, CH_3), 5.68 (s, 1H, CH), 6.57-7.88 (m, 8H, Ar-H), (m, 2H, CH=CH), 8.12 (s, 2H, NH_2)	44.72 (C_{19}, C_{20}), 63.34 (C_1), 116.52 (C_{12}), 121.55-134.42 (C_2-C_9),(C_{13}-C_{18}), 159.51(C_{10},C_{11}).
2	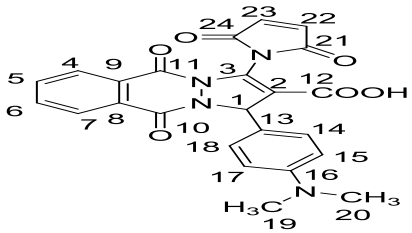	3.28 (s, 6H, CH_3), 5.56 (s, 1H, CH),6.65-7.87 (m, 8H, Ar-H), (m, 2H, CH=CH), ١١.34 (s, 1H, OH).	45.21(C_{19}, C_{20}), 58.36 (C_1), 122.34-137.81(C_2-C_9),(C_{13}-C_{18}), (C_{22},C_{23}), 161.35 (C_{10},$C_{11,}$ C_{21},C_{24}), 169 (C_{12}).
3	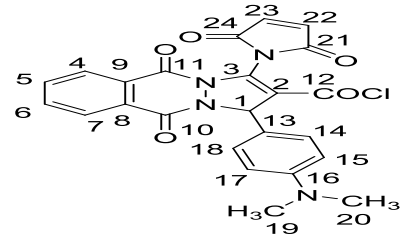	3.36 (s, 6H, CH_3), 5.71 (s, 1H, CH), 6.66-7.91 (m, 8H, Ar-H), (m, 2H, CH=CH).	46.11 (C_{19}, C_{20}), 59.82 (C_1), 120.66-136.90 (C_2-C_9),(C_{13}-C_{18}), (C_{22},C_{23}), 162.33 (C_{10},$C_{11,}$ C_{21},C_{24}), 168.44 (C_{12}).
4	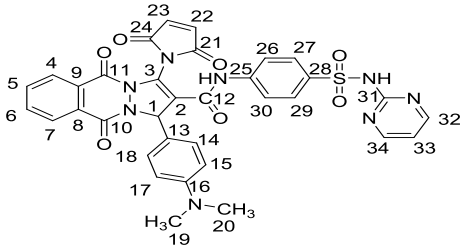	3.41 (s, 6H, CH_3), 5.61 (s, 1H, CH), 6.95-8.12 (m, 15H, Ar-H), (m, 2H, CH=CH), 9.44 (s, 1H, -CO-N<u>H</u>), 11.21 (s, 1H, -SO_2-N<u>H</u>).	44.35 (C_{19}, C_{20}), 58.33 (C_1), 118.11-139.44 (C_2-C_9),(C_{13}-C_{18}), (C_{22},C_{23}), (C_{25}-C_{34}), 167.81 (C_{10},$C_{11,}$ $C_{12,}$$C_{21}$,$C_{24}$),
5	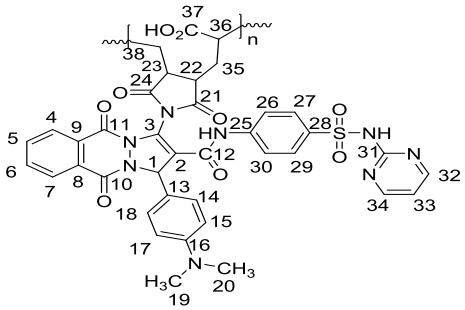	1.81 (m, nH, CH_2), 3.21 (s, 6H, CH_3), 3.59 (s, 2H, CH), 6.70-8.18 (m, 15H, Ar-H), 9.67 (s, 1H, -CO-N<u>H</u>),10.24 (s, OH),11.33 (s, 1H, -SO_2-N<u>H</u>)	35.44 (C_{35}, C_{36} ,C_{38}), 45.83 (C_{22},C_{23}), 48.66 (C_{19}, C_{20}), 61.44 (C_1), 120.57-139.89 (C_2-C_9),(C_{13}-C_{18}), (C_{25}-C_{34}), 165.22 (C_{10},$C_{11,}$ $C_{12,}$$C_{21}$,$C_{24}$), 171.34 ($C_{37}$).
	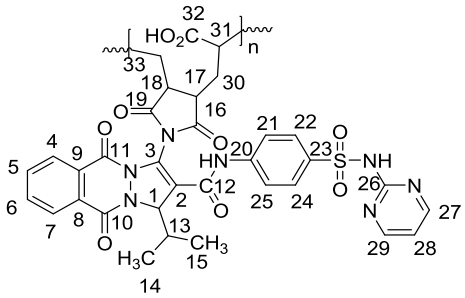	1.88 (m, nH, CH_2), 3.26 (s, 3H, CH_3), 3.63 (s, 2H, CH), 6.77-8.25 (m, 11H, Ar-H), 9.71 (s, 1H, -CO-N<u>H</u>),10.90 (s, OH), 11.29 (s, 1H, -SO_2-N<u>H</u>)	36.21 (C_{30}, C_{31} ,C_{33}), 40.17 (C_{17},C_{18}), 43.79 (C_{14}, C_{15}), 62.12 (C_1), 122.33-138.31 (C_2-C_9), (C_{20}-C_{29}), 164.22 (C_{10},$C_{11,}$ $C_{12,}$$C_{16,}$$C_{19}$), 171.34 ($C_{32}$).

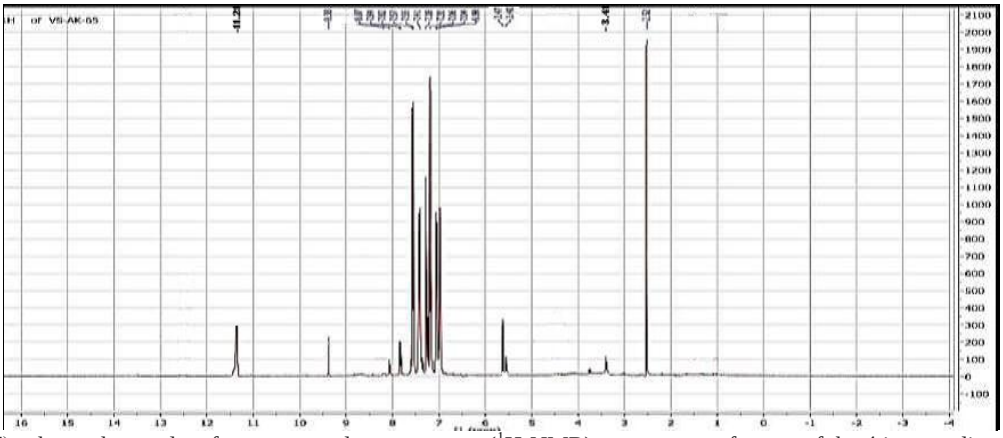

Fig. (7) shows the results of a proton nuclear resonance (^{1}H-NMR) spectrometer for one of the **4** intermediate compound.

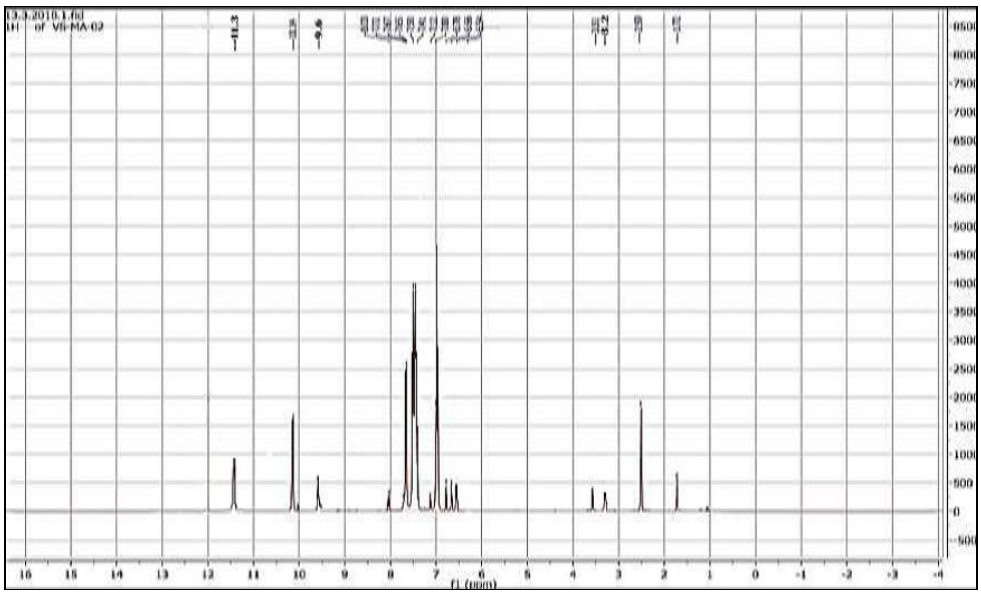

Fig. (8) Demonstrates the results of a proton nuclear resonance spectroscopy (^{1}H-NMR) for one of the final compound **5**.

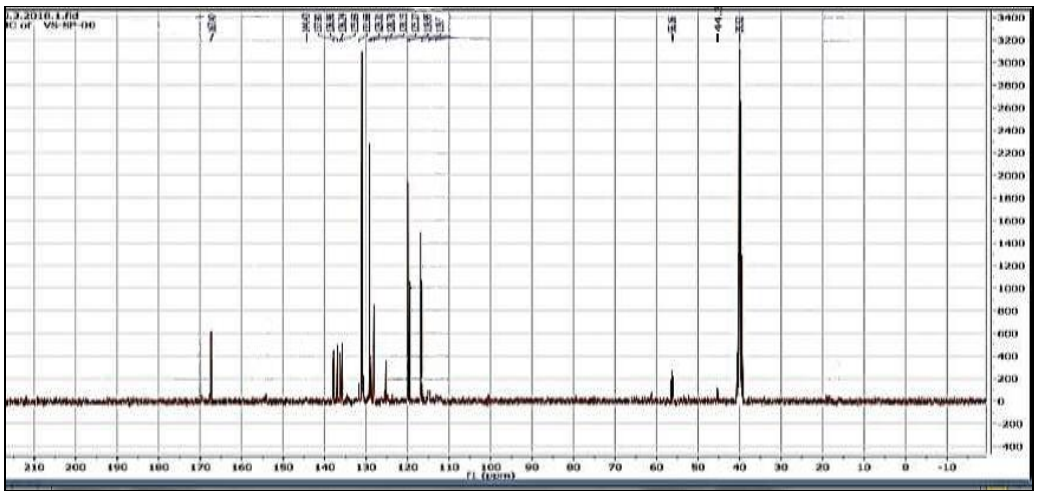

Fig. (9) shows the results of the carbon nuclear resonance resonance spectroscopy (13C-NMR) for one of the **4** intermediate.

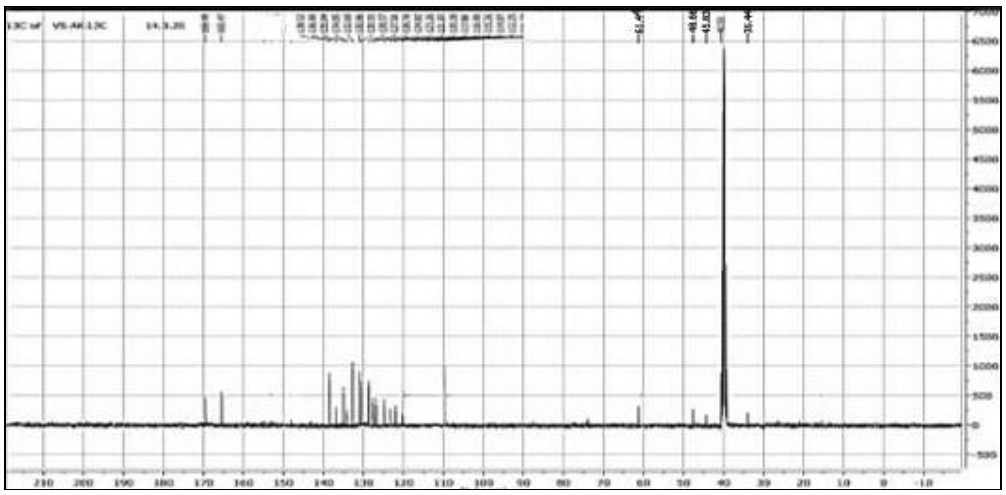

Fig. (10) shows the results of the carbon nuclear resonance spectroscopy (13C-NMR) for one of the final compound **5.**

3.3 Antibacterial activity

Two Gram-positive Bacteria Staphylococcus aureus and Bacillus subtilis and two Gram-negative Bacteria E. coli, and *Pseudomonas aeruginosa* were used to test the antibacterial activity of the **3-6** compounds. The results were obtained by the well-diffusion method using a 60 mg 10 mL^{-1} concentration (in DMSO) with a volume of 50 µL per well. The results are tabulated in table 5 using DMSO as a negative control while Tetracycline was used as positive control. Compound **3** exhibited lower antibacterial activity against Gram-positive bacteria then tetracycline with IZD of 10–14 mm. compound **4** exhibit activity against Gram-positive and only one Gram-negative bacteria *Escherichia coli* 12-18 mm. **5**, all tested Gram-positive and Gram-negative bacteria exhibited antibacterial activity against all tested Gram-positive and Gram-negative bacteria. The efficiency of compound **6** against all tested micro-organisms is good with IZD 8-22 mm. compound **6** was chosen for further studies because of its higher IZD values The compound **4** did not show any antibacterial activity against *Pseudomonas aeruginosa*, and tetracycline controls showed high antibacterial activity against all tested bacterial species with inhibition zone diameter (IZD) of 14-18. Table (4), Fig. (11) and (12).

Table (4): Shows in vitro antibacterial activity data (inhibition zone diameter (IZD) in mm) for compounds **3, 4,5** and **6**, the concentration was 60 mg 10mL^{-1} in DMSO (6 g L^{-1}).

Compounds No.	*Staphylococcus Aureus*	*Bacillus subtilis*	*Escherichia coil*	*Pseudomonas aeruginosa*
3	14	10	10	14
4	18	12	13	0
5	17	14	12	8
6	18	22	14	8
DMSO	0	0	0	0
Tetracycline	18	14	18	16

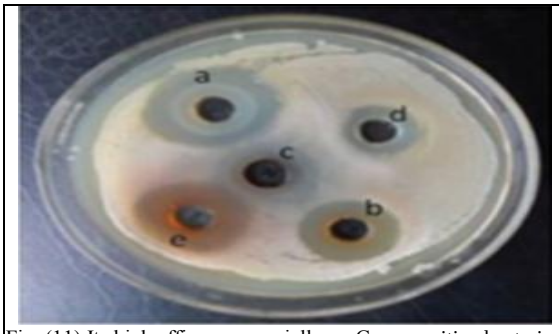

Fig. (11) Its high efficacy, especially on Gram-positive bacteria (Bacillus subtilis), for intermediate and final compounds

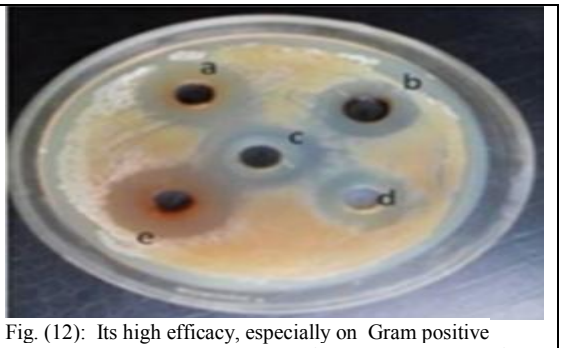

Fig. (12): Its high efficacy, especially on Gram positive bacteria (Staphylococcus Aureus), for intermediate and final compounds.

4. Conclusion

Preparing new polymers linked with heterocyclic rings that can be used in different industries in different industries, such as pharmaceutical industries, by using nanoxides extracted from natural sources. It is known that the green synthesis of ZnONPs is much safer and environmentally friendly as compared to chemical synthesis.

Initial pharmacokinetic evaluation of some of these manufactured polymers. Compounds **1-6** were prepared, and their chemical compositions proved. Most of the synthesized compounds showed inhibitory effects on the growth of bacteria outside the body of the organism on culture media compared to the standard medicine used as standard

Acknowledgements

This work was grateful supported by College of Remote sensing and Geophysics, Al-Karkh University for Science, and department of chemistry, college of science for women, Baghdad University, Iraq.

5. References

1- Rajakumar, Govindasamy ,*et al.* "Green approach for synthesis of zinc oxide nanoparticles from Andrographis paniculata leaf extract and evaluation of their antioxidant, anti-diabetic, and anti-inflammatory activities" *Bioprocess and Bio Systems Engineering* 41,no.1(2018):21-30.

2. Al-Sahib, Sanaa, *et al.* "Synthesis, Characterization of Organic Nanoparticles of Oxadiazole Derivatives" *Journal of Physics: Conference Series*, 1294,no.5(2019): 052024.

3. Mishra, Pawan K *et al.* "Zinc oxide nanoparticles: a promising nanomaterial for biomedical applications" *Drug Discovery Today*, 22, no. 2 (2017): 1825–1834.

4. Kołodziejczak-Radzimska, Agnieszka and Jesionowski, Teofil "Zinc oxide–from synthesis to application: a review" *Materials***,** 7, no.4(2014): 2833–2881.

5. Elumalai, K and Velmurugan, Sivasangari "Green synthesis, characterization and antimicrobial activities of zinc oxide nanoparticles from the leaf extract of Azadirachta indica (L.)" *Applied Surface Science*, 345, (2015):329–336.

6. Shagufta, Bi *et al*. "Antimicrobial resistance and typing of Salmonella isolated from street vended foods and associated environment" *Journal of Food Science and Technology*, 54, no.8(2017): 2532-2539.

7. Mahendra, C *et al.* "Antibacterial and antimitotic potential of bio-fabricated zinc oxide nanoparticles of *Cochlospermum religiosum* (L.)" *Microbial Pathogenesis*, 110, (2017):620–629.

8. Fu, Li *and Fu, Zhuxian "Plectranthus amboinicus* leaf extract-assisted biosynthesis of ZnO nanoparticles and them photocatalytic activity" *Ceramics International*, 41, no. 2(2015): 2492–2496.

9. Ali, Khursheed *et al.* "Aloe Vera extract functionalized zinc oxide nanoparticles as nanoantibiotics against multi-drug resistant clinical bacterial isolates" *Journal of Colloid and Interface Science*, 472, (2016): 145–156.

10. Raauf, Ayad MR, *et al.* "Synthesis, characterization and antimicrobial study via new heterocyclic derivatives of trimethoprim" *Natural product research,* 33,no.9(2019):1277-1283.

11. Yuvakkumar, R *et al.* "Novel green synthetic strategy to prepare ZnO nanocrystals using rambutan (*Nephelium lappaceum* L.) peel extract and its antibacterial applications" *Materials Science and Engineering*, 41, (2014): 17–27.

12. Janaki, A Chinnammal *et al.* "Synthesis, characteristics and antimicrobial activity of ZnO nanoparticles" *Spectrochimica Acta Part A: Molecular and Biomolecular Spectroscopy*, 144, (2015): 17–22.

13. AL-Tamimi, Entesar Obeed *et al.* "Synthesis, Characterization and Antibacterial Studies of 2-azetidinones Compounds Derived from Amoxicillin" *Al-Mustansiriyah Journal for Pharmaceutical Sciences,* 15,no.1(2015):14-2.

14. Sharma, Deepali *et al.* "Biosynthesis of ZnO nanoparticles using *Jacaranda mimosifolia* flowers extract: synergistic antibacterial activity and molecular simulated facet specific adsorption studies" *Journal of Photochemistry and Photobiology B: Biology*, 162(2016):199–207.

15. Sharma, Harshita *et al.* "Development and characterization of metal oxide nanoparticles for the delivery of anticancer drug" *Artificial Cells, Nanomedicine, and Biotechnology*, 44, no. 2(2016): 672–679.